NASA/TP–2010-216722

OLTARIS: On-Line Tool for the Assessment of Radiation in Space

Robert C. Singleterry, Jr., Steve R. Blattnig, Martha S. Clowdsley, Garry D. Qualls, Christopher A. Sandridge, Lisa C. Simonsen, and John W. Norbury
NASA Langley Research Center, Hampton, Virginia

Tony C. Slaba and Steven A. Walker
Old Dominion University, Norfolk, Virginia

Francis F. Badavi
Christopher Newport University, Newport News, Virginia

Jan L. Spangler
Lockheed Martin Operations Support, Hampton, Virginia

Aric R. Aumann
Analytical Services and Materials, Inc., Hampton, Virginia

E. Neal Zapp, Robert D. Rutledge, and Kerry T. Lee
NASA Lyndon B. Johnson Space Center, Houston, Texas

Ryan B. Norman
University of Tennessee, Knoxville, Tennessee

July 2010

NASA STI Program . . . in Profile

Since its founding, NASA has been dedicated to the advancement of aeronautics and space science. The NASA scientific and technical information (STI) program plays a key part in helping NASA maintain this important role.

The NASA STI program operates under the auspices of the Agency Chief Information Officer. It collects, organizes, provides for archiving, and disseminates NASA's STI. The NASA STI program provides access to the NASA Aeronautics and Space Database and its public interface, the NASA Technical Report Server, thus providing one of the largest collections of aeronautical and space science STI in the world. Results are published in both non-NASA channels and by NASA in the NASA STI Report Series, which includes the following report types:

- TECHNICAL PUBLICATION. Reports of completed research or a major significant phase of research that present the results of NASA programs and include extensive data or theoretical analysis. Includes compilations of significant scientific and technical data and information deemed to be of continuing reference value. NASA counterpart of peer-reviewed formal professional papers, but having less stringent limitations on manuscript length and extent of graphic presentations.

- TECHNICAL MEMORANDUM. Scientific and technical findings that are preliminary or of specialized interest, e.g., quick release reports, working papers, and bibliographies that contain minimal annotation. Does not contain extensive analysis.

- CONTRACTOR REPORT. Scientific and technical findings by NASA-sponsored contractors and grantees.

- CONFERENCE PUBLICATION. Collected papers from scientific and technical conferences, symposia, seminars, or other meetings sponsored or co-sponsored by NASA.

- SPECIAL PUBLICATION. Scientific, technical, or historical information from NASA programs, projects, and missions, often concerned with subjects having substantial public interest.

- TECHNICAL TRANSLATION. English-language translations of foreign scientific and technical material pertinent to NASA's mission.

Specialized services also include creating custom thesauri, building customized databases, and organizing and publishing research results.

For more information about the NASA STI program, see the following:

- Access the NASA STI program home page at *http://www.sti.nasa.gov*

- E-mail your question via the Internet to help@sti.nasa.gov

- Fax your question to the NASA STI Help Desk at 443-757-5803

- Phone the NASA STI Help Desk at 443-757-5802

- Write to:
  NASA STI Help Desk
  NASA Center for AeroSpace Information
  7115 Standard Drive
  Hanover, MD 21076-1320

NASA/TP–2010-216722

OLTARIS: On-Line Tool for the Assessment of Radiation in Space

Robert C. Singleterry, Jr., Steve R. Blattnig, Martha S. Clowdsley, Garry D. Qualls, Christopher A. Sandridge, Lisa C. Simonsen, and John W. Norbury
NASA Langley Research Center, Hampton, Virginia

Tony C. Slaba and Steven A. Walker
Old Dominion University, Norfolk, Virginia

Francis F. Badavi
Christopher Newport University, Newport News, Virginia

Jan L. Spangler
Lockheed Martin Operations Support, Hampton, Virginia

Aric R. Aumann
Analytical Services and Materials, Inc., Hampton, Virginia

E. Neal Zapp, Robert D. Rutledge, and Kerry T. Lee
NASA Lyndon B. Johnson Space Center, Houston, Texas

Ryan B. Norman
University of Tennessee, Knoxville, Tennessee

National Aeronautics and
Space Administration

Langley Research Center
Hampton, Virginia 23681-2199

July 2010

Acknowledgments

This work was supported by the Human Research Program in the Advanced Capabilities Division under the Exploration Systems Mission Directorate and performed by the members of the Design Tool Project in the Space Radiation Program Element.

Available from:

NASA Center for AeroSpace Information
7115 Standard Drive
Hanover, MD 21076-1320
443-757-5802

Contents

List of Figures

List of Tables

Acronyms

OLTARIS	On-Line Tool for the Assessment of Radiation In Space
AP8MAX	Aerospace corporation Proton version 8 at solar MAXimum
AP8MIN	Aerospace corporation Proton version 8 at solar MINimum
CAD	Computer Aided Design
CAF	Computerized Anatomical Female
CAM	Computerized Anatomical Male
CSDA	Continuous Slowing Down Approximation
DSNE	Design Specification for Natural Environments
EO	Earth Orbit
FAX	Female Adult voXel phantom
GCR	Galactic Cosmic Ray
HZETRN2005	High Z and Energy TRaNsport 2005 - basic particle transport code used in OLTARIS
ICRP	International Commission on Radiological Protection
IGES	Initial Graphics Exchange Specification
ISS	International Space Station
ITAR	International Traffic in Arms Regulations
LEO	Low Earth Orbit
LET	Linear Energy Transfer
MAX	Male Adult voXel phantom
MC	Monte Carlo
NCRP	National Council on Radiation Protection
NUCFRG2	NUClear FRaGmentation Version 2 - basic heavy ion cross sections used in OLTARIS
SGE	Sun Grid Engine
SIREST	Space Ionizing Radiation Environment and Shielding Tools
SPE	Solar Particle Event
STS	Space Transportation System - shuttle
TEPC	Tissue Equivalent Proportional Counter
TLD-100	lithium-fluoride Thermo-Luminescent Detector version 100

Nomenclature

Dose	amount of energy deposited into a certain quantity of material
Dose Equivalent	tissue dose converted to biological effects in humans - ICRP-60
Effective Whole-Body Dose Equivalent	organ weighted dose equivalent - NCRP-132
m	proton mass, $1.67 \times 10^{-27}\mathrm{kg}$ or $938\,\mathrm{MeV}$
E	particle *kinetic* energy per mass unit, $\frac{\mathrm{MeV}}{\mathrm{amu}}$ or AMeV
ϕ	differential particle flux or fluence, $\frac{\#}{\mathrm{cm}^2-\mathrm{AMeV}-[\mathrm{day\ or\ event}]}$
$Q_{\mathrm{ICRP}-60}$	quality factor to multiply by energy deposited (dose) to calculate a human response (dose equivalent), $\frac{\mathrm{Sv}}{\mathrm{Gy}}$

Executive Summary

The On-Line Tool for the Assessment of Radiation In Space (OLTARIS) is a World Wide Web based tool that assesses the effects of space radiation on humans and electronics in items such as spacecraft, habitats, rovers, and spacesuits. This document explains the basis behind the interface and framework used to input the data, perform the assessment, and output the results to the user as well as the physics, engineering, and computer science used to develop OLTARIS. The transport and physics is based on the HZETRN2005 and NUCFRG2 research codes. The OLTARIS website is the successor to the SIREST website from the early 2000's. Modifications have been made to the code to enable easy maintenance, additions, and configuration management along with a more modern web interface. Overall, the code has been verified, tested, and modified to enable faster and more accurate assessments.

The interface and data input/output are based on user needs determined through user interviews and the creation of *use cases*. The code is broken down into five basic elements: Radiation Environment (Boundary Conditions), Material Properties, Geometry (slab or vehicle thickness distributions), Transport, and Response Functions. The path through these elements and the data input/output is based on the use case being executed. As new use cases are created, only the code necessary to complete each use case is generated (code is reused), the web interface is updated for the new functionality, and new web scripts are created to tie the assessment together.

All code is tested with module and functional testing. These tests are updated whenever new use cases are implemented. If any code is changed or added, the whole system is tested to make sure functionality is not compromised and the test answers do not change in an unintended manner over time. This continuous verification is an important part of OLTARIS. It ensures reliability over time even as modifications and improvements are made to ensure state-of-the-art predictions.

As new use cases are generated, new algorithms are also needed to implement them. Currently under development is a ray-by-ray calculation, which will allow any number of materials in any order to be analyzed in a spacecraft geometry. Other new use cases can be added as needs dictate. The next major areas of modification are more accurate transport algorithms, better uncertainty estimates, and electronic response functions. Improvements in the existing algorithms and data occur continuously and are logged in the change log section of the website.

1 Introduction and Background

Particle transport algorithms and methods needed to assess the radiation shielding in spacecraft are difficult to solve and master. When non-experts are asked to utilize them in their normal work flow, the functionality of these algorithms and methods needs to be simple, clear, and straightforward. The answers that they give need to be accurate, characterized by an uncertainty, and reproducible [1, 2]. Achieving these goals entails numerous characteristics: modularity, version control, modern user interface, maintainability, verification, and validation. Data interfaces and formats need to be established between modules, clear paths need to be established for data flow, and user interfaces need to feed the proper data into and out of the system so that a non-expert user can understand the input and results.

The SIREST website [3] attempted to enable this type of functionality for space radiation analysis. OLTARIS, its successor, contains improved methods for handling complex geometries and an increased level of code verification and manageability. The URL is listed as https://oltaris.larc.nasa.gov/. The first task was to establish acceptable user interactions with the website. This was achieved through interviewing potential users about how they envisioned working with this type of data. Use cases were generated to capture this desired work flow and functionality. From these initial use cases and other programmatic requirements, an initial capability was defined.

Current, state-of-the-art, research-based radiation analysis tools were identified and utilized in the construction of OLTARIS. The research-based particle radiation transport code HZETRN2005 [4, 5] is the basis for OLTARIS. HZETRN2005 has embedded response functions that were greatly expanded in OLTARIS. New response functions not in HZETRN2005 were also added. The NUCFRG2 [6, 7, 8] code was used for heavy ion cross sections with HZETRN2005 embedded light ion cross sections [9]. The rest of the paper will describe the current capability and how that capability was implemented within OLTARIS.

2 OLTARIS Description and Functionality

The OLTARIS architecture is divided into two main parts, the website, on which users interact through a browser, and the execution environment, where the computations are performed. This architecture enables maximum flexibility and is scalable as demand increases. The website is built primarily with standard open source components. The core is Ruby on Rails [10] with a MySQL [11] database running on an Apache [12] web server. The only licensed, server-side component is an Adobe Flash plugin which allows the users to plot and examine results using a standard, free plugin that most browsers already have.

The execution environment is primarily FORTRAN executables tied together with some Perl and Ruby scripts running on a computational cluster. Data is passed between the web server and the cluster using XML files. Jobs are managed with the open-source Sun Grid Engine (SGE) [13]. There are benefits to having SGE serve as a mediator between the user interface and

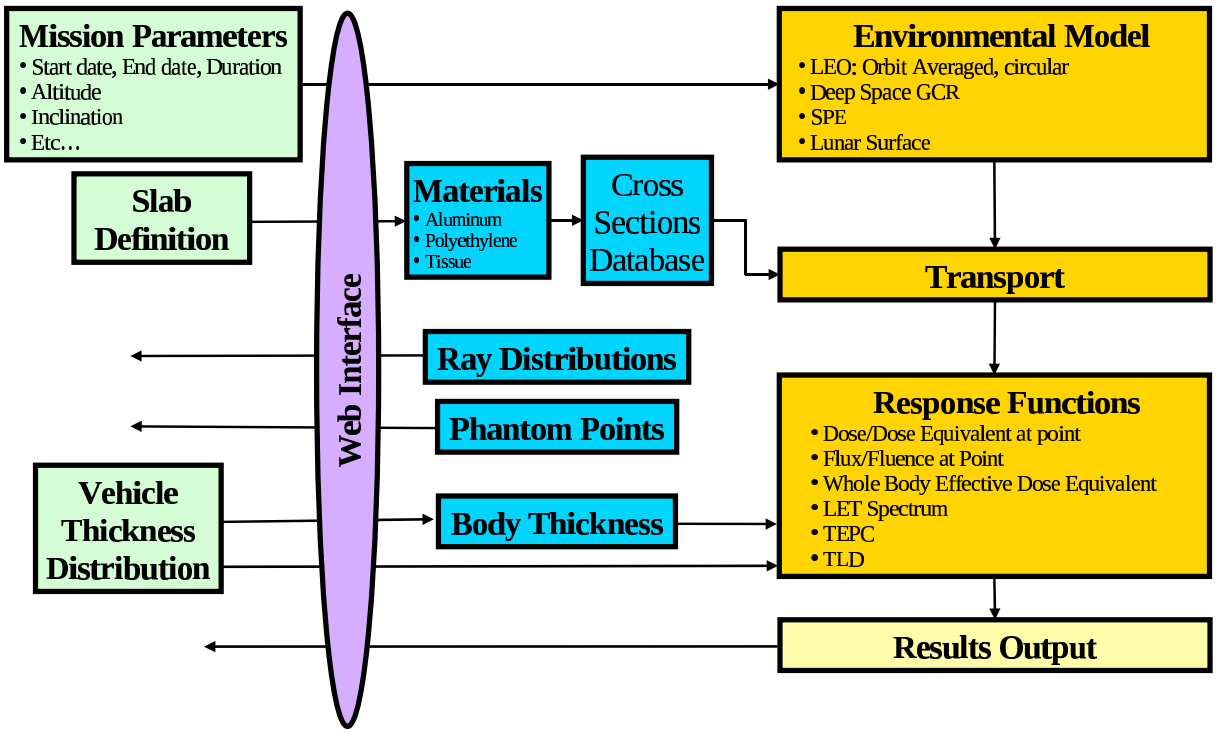

Figure 1: Program Flow for OLTARIS

the computations. First, additional nodes or clusters can be easily added as demand increases. Also, the web interface can easily be replaced with a desktop client sometime in the future, if requirements dictate.

Figure 1 shows the program and data flow for OLTARIS. The boxes indicate different components or modules of the system. This modular system makes it easy to maintain and upgrade as new algorithms, methods, and capabilities are developed. Each module has a clearly defined input and output data format so that the individual module developers don't have to know about the coding details of the other modules; however, they can easily interface with all the other modules they need. For example, if requirements dictate the development of another radiation environment, the new radiation environment will plug into the process cleanly, as long as its outputs are in the same format as every other environment model.

The green boxes indicate the data that the user needs to supply: a slab definition or a thickness distribution of their vehicle (see Section 2.2), and mission parameters that will determine how the external radiation environment is computed. The blue boxes indicate data that the user can either download from the web server or data used in the calculations and stored on the execution host. This includes material data with associated cross section databases (see Section 3) and body-thickness distributions used in the calculation of whole-body effective dose equivalent. The downloadable content includes ray distributions and a phantom human CAD (Com-

puter Aided Design) object that can be used to prepare the vehicle thickness distributions. The gold boxes represent the computations which are performed on the execution host and consist of three modules: the environmental model, the particle transport, and the response functions.

The environment module is where the external radiation environment is computed. The user can currently choose from four different types of environments: an historic Solar Particle Event (SPE) or a linear combination of SPEs, free-space Galactic Cosmic Rays (GCR), Lunar Surface, or Earth Orbit (EO). The output of these environments is a spectral flux or fluence. The units are $\frac{\text{particles}}{\text{cm}^2-\text{AMeV}-\text{time}}$, where $time$ is given in events for SPE (fluence) and days for GCR and EO (flux). This flux/fluence is then used as the boundary condition for the transport. More details about the environments can be found in Section 4.

The transport module is composed of two paths depending on the type of geometry the user selects, either slab or thickness distribution. Both paths use nuclear transport methods based on HZETRN2005, which have been greatly improved, verified, and validated [14, 15, 16, 17, 18, 19]. The slab computation transports particles from the chosen boundary condition, through any user defined materials and thicknesses, to generate fluxes/fluences at the material interfaces and at the end boundary. The computation for the case of a thickness distribution is a series of transport runs for an array of depths for each material that the user needs. OLTARIS currently supports aluminum, polyethylene, and tissue for possible materials in a vehicle. The output is an array of flux/fluence versus energy and thickness for every combination of material thicknesses. The selection of the spatial grid (thickness intervals) and the energy grid is dependent on the boundary condition and is not user selectable at this time. Further details about the transport method can be found in Section 5.

The response function module takes the resulting flux/fluence calculated with the transport module and computes selected responses for each depth of the various materials and the total responses at the end of the slab or at the selected vehicle location. For thickness distributions, an array of response function versus depth curves are computed for the same set of material spatial grids selected for the flux/fluence transport. Total quantities along each ray in the thickness distribution are calculated by interpolating over the response function versus depth database just computed. The total quantity at a target point is then calculated by integrating over all of the rays. In the case of whole body effective dose equivalent (or *effective dose*), an added step is performed to combine the vehicle thickness distributions with the body thickness distributions for a large number of target points in a human phantom. The process for calculating dose equivalent at a single target point is then repeated for each body target point and a weighted average of these values is taken. Details about all the possible responses can be found in Section 6. Finally, all the results are transferred back to the user's account on the website for viewing, plotting, or download.

2.1 Web interface

Users need to register on the OLTARIS website and receive approval before they can enter the website. This is required because some of the content falls under the purview of the Interna-

tional Traffic in Arms Regulations (ITAR) [20], but registration also allows for regulating and maintaining limited computer resources by permitting only those with a real need and knowledge to access the site. Once the user account has been activated by a site administrator, the user can login and start using the tools.

The first page the user sees after login is the *Projects* page. Each project is the complete encapsulation of a calculation; it includes the definition of the radiation environment, the selection of a thickness distribution or slab, and a selection of desired responses. This page allows the user to create new projects, edit existing projects, submit new jobs to the compute cluster, and access the results of previous jobs. A job is an instantiation of a project that is packaged for processing. When a new project is created, the user is stepped through a series of pages that allows the user to define the different aspects of the problem. Help pages are available at any point in the process if the user needs more information. Once the project is saved, the user is returned to the *Projects* page and can submit a job to the compute cluster. A project can include multiple jobs so that if the user wants to change particular elements of the project, say select a different environment or response, the user can do so and create an additional job that can be submitted under that same project.

Once a job is submitted, the user can check its status from the *Jobs* page for a particular project. When a job is complete, an email is sent to the user from the grid scheduler (SGE) and the user can view the results by selecting *Display/Download Results* for the completed job on the *Jobs* page. The results page will list some of the results directly in tabular form and allow the user to plot data, such as dose versus depth curves and flux/fluence data. The plot page has the option to copy the plotted data to the user's clipboard so that it can be pasted into various local applications on their computer. The user also has the option to download the data to their desktop computer in the form of a text file or can cut-and-paste directly into EXCEL™.

Another section of the website is the *Thickness Distributions* page which is selected from one of the main tabs across the top of the page. This page presents a list of the user's current thickness distributions and allows the user to upload new ones. Once a thickness distribution is uploaded to the site, it is available for selection from a project page. Thickness distributions are uploaded to the site in the form of an XML file. A document describing the format of the file and sample files can be downloaded from the *Thickness Distributions* page. The user can also download a phantom CAD object that represents a human geometry. This can be positioned and oriented in the user's CAD model to help select the proper target points in their vehicle geometry and compute effective dose responses. The next section of this paper describes this process in more detail.

The *Slabs* and *Materials* sections, selected from the tabs at the top of each page, are used to create user-defined slabs of any material the user desires. The user first defines the materials they want to use at the *Materials* tab by entering the material's elemental mass percentage, its molecular mass percentage, or its chemical formula. Once the material is defined, the user can submit the material definition to the computational grid so that the material cross sections (see Section 3) can be computed for later use. Once the cross section database is available, the user can then go to the *Slabs* tab and define a layup of materials of any thickness, in any order the

user chooses. This capability is useful for comparing new material or structural concepts. Once a slab is created, it can be selected for a project from the *Projects* page.

The previous discussion describes the current layout of the website; however, the developers are continuing to add content and update models, so a *Change Log* is accessible from each page to communicate any changes or updates to the site or its underlying code/data. There are also links on each page to send an email to the developers to offer suggestions or report problems. Feedback from users is encouraged and is very important in prioritizing new capabilities.

2.2 Thickness Distributions

In order to compute a response in a realistic vehicle geometry, a representation of the vehicle geometry, in the form of a material thickness distribution, is required. This thickness distribution is computed using a process called ray tracing. Ray tracing uses a directionally distributed set of rays emanating from the same point to determine how much material is surrounding that point in each ray direction. The point source of the rays is commonly called a *target point*. The intersections of the rays and the various components of the vehicle CAD model are used to determine the along-the-ray thicknesses of the components, which are stored along with their associated material types.

OLTARIS currently supports only three materials - aluminum, polyethylene, and human tissue in vehicle geometries, as mentioned previously. For example, one ray could intersect a human being, which would be a thickness of tissue, followed by some shielding material, such as polyethylene, and then the vehicle structural components, which could be a thickness of aluminum. Rays typically intersect multiple objects, so there can be many separate material thicknesses along each ray. The current version of OLTARIS will sort and combine these thicknesses so that the outermost layer of shielding is composed of all the collected aluminum thicknesses along that ray, the next layer of shielding represents the total thickness of polyethylene along that ray, and the innermost layer represents the total amount of tissue along that ray.

Any angular distribution of rays may be used, as long as they are distributed evenly enough that each ray can approximately represent an equal solid angle of shielding surrounding its target point. However, to compute an effective whole-body dose equivalent using OLTARIS, the user will need to use one of the many ray distributions that are available for download from the Thickness Distributions page. Those currently available include distributions with 42, 492, 512, 968, 1002, 4002, 9002, or 10,000 rays. If the user needs to take into account a specific body phantom orientation with respect to their vehicle, OLTARIS provides a process that makes this possible.

To calculate an effective dose, OLTARIS combines uploaded vehicle thickness distributions with pre-computed body phantom thickness distributions. The process used to combine these distributions provides the ability to analyze a specific body orientation relative to a vehicle shielding model and the ability to capture the local variation of radiation intensity inside the vehicle. This local variation could be due to variations in the amount of shielding surrounding

different regions of the vehicle interior and might, for example, yield a situation in which the phantom's head is less shielded than its feet.

In order to accurately represent the user's desired phantom orientation within a vehicle model, the user will need to download one of two specially developed CAD models from the OLTARIS web site. These CAD models are proxies for the male and female body phantoms that are available for use in OLTARIS. The user will need to load this model into their CAD software, as a new component in their shielding model. The models have been made available in an IGES (Initial Graphics Exchange Specification) file format to gain broad compatibility with the widest possible array of CAD software. Each body phantom proxy CAD model includes eight reference points.

The three points used to establish the phantom orientation have been colored green and labeled "A", "B", and "C" (see Figure 2). Once oriented, the user will record the (x, y, z) coordinates of these three points, taking care to use the same reference coordinate system that will be used for ray tracing. The coordinates of these three points can be entered into a form on the OLTARIS website to generate a custom ray distribution, rotated to take into account the phantom orientation. The form used to create these ray distributions can be accessed from the Thickness Distributions page. The user should use this ray distribution to ray trace vehicle thickness distributions that correspond to that phantom orientation.

The other five reference points included with each IGES phantom proxy are colored red and are used to capture the effects of shielding variation within the vehicle interior. These five points correspond to five body zones, as shown in Figure 2. To use this feature, the user will need to perform five separate vehicle ray traces and calculate five separate vehicle thickness distributions, each centered on one of the red zone target points. The effective whole-body dose equivalent calculation (see Section 6.6) within OLTARIS uses tissue thickness distributions based upon hundreds of target points that are distributed throughout the body phantom in specific tissues. OLTARIS will add the vehicle thickness distribution closest to each of the zone's tissue thickness distributions to get the total shielding around each body point. The user does not have to use five target points. One target point can be used; therefore, all of the body points are added to the single vehicle thickness distribution. However, a single target point will be less accurate than the five target point case, as the local variations in the vehicle shielding may be significant.

2.3 Verification

Users expect to get reliable and accurate results from the tool sets that they use; therefore, OLTARIS has implemented several levels of verification to ensure consistent and accurate results. The OLTARIS system consists of thousands of lines of code, hundreds of files, and megabytes of data. All of the source code and data are stored in a version-control repository that all of the developers can access. This way, all changes are tracked and everyone can have access to the same code base. The source repository is organized along the lines of Figure 1 and each box has a specific developer who is responsible for, or *owns,* that module. Before any new methods or techniques are stored in the repository, the developer must ensure the accuracy

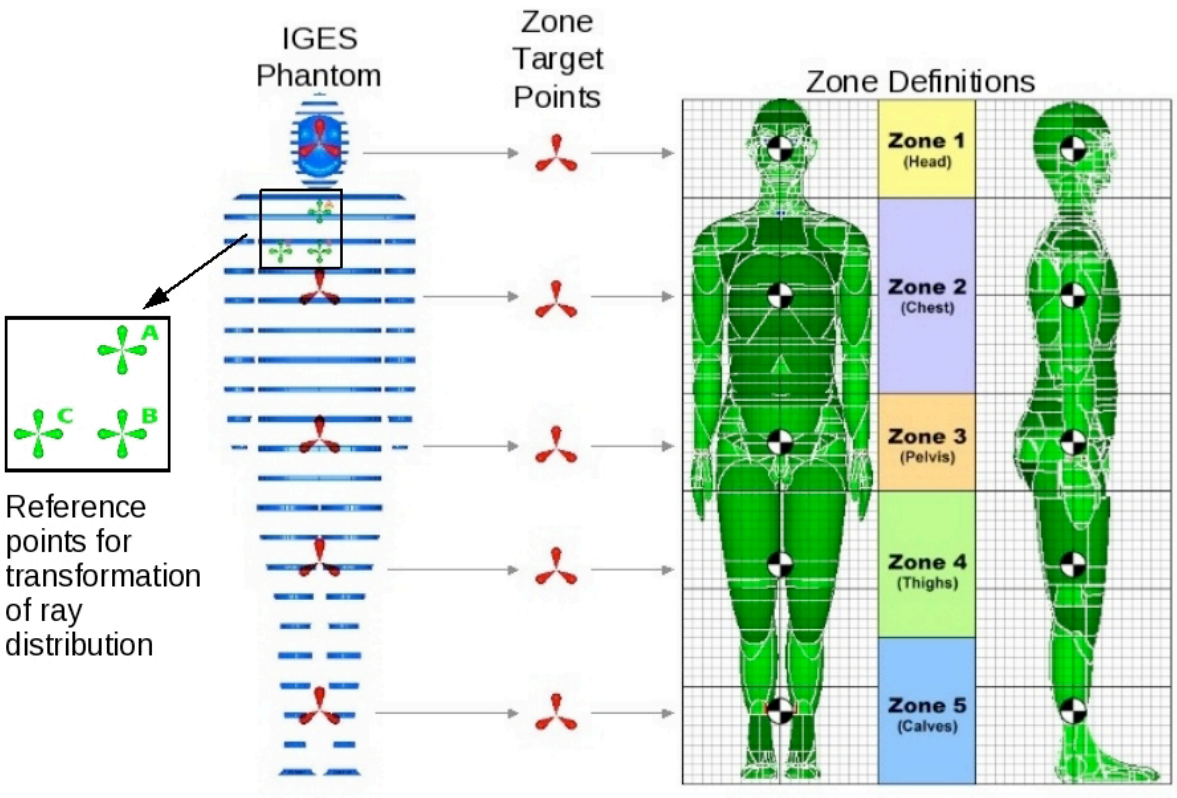

Figure 2: Body Phantom Zone Points

of the method and write corresponding test cases that are also entered into the repository. These test cases are referred to as *module tests.* Test cases are also developed that test the interaction between modules or complete runs through the system; these are called *functional tests.* The combination of module and functional tests are intended to verify that the code base and data are generating consistent results. This suite of tests is automatically re-run periodically to make sure that any changes entered into the repository do not break the system somewhere else. If a discrepancy is found, the responsible developer is notified and fixes the problem. Once the code has been sufficiently tested and is ready to be deployed, it is *tagged* or labeled for reference. This tagged version is a snapshot of the code base and the tagged version number is noted at the bottom of every page on OLTARIS.

The web code is maintained under version control, but the testing is manual. There is both a test website and a production website. The test site has its own server, database, and execution environment, but it is only used by the developers. Projects can be set up and run on the test website and compared to runs made without the web code. Several developers test different paths in order to be sure everything is working properly. Once everything is working properly on the test system, the codes are deployed to the production site. There is also a *change log*

on OLTARIS so that users can see when changes and updates are made that may change their results.

3 Material Properties

Material properties are an important part of the transport algorithm. Material dependent cross sections are used to predict the ways in which neutrons and charged particles will interact with shielding material. For vehicle thickness distributions, three materials (currently aluminum, polyethylene, and tissue) are used and their cross sections are pre-calculated. For slab based calculations, the user can input materials in numerous ways. These materials are then available for use in a pull-down list when defining slabs. Pre-defined materials important to the space radiation community already exist in the pull-down menus upon first time use.

A material cross section is the probability of interaction between a particle projectile and the target nucleus with a particular outcome of that interaction. This probability is represented as the effective cross sectional area of the target nucleus as a function of the projectile energy and particle type. The unit is cm^2 and is usually represented as a barn or $10^{-24}\mathrm{cm}^2$. An example of an interaction would be:

$$^{56}\mathrm{Fe} + {}^{27}\mathrm{Al} \longrightarrow {}^{12}\mathrm{C} + {}^{\mathrm{A}}_{\mathrm{Z}}\mathrm{X}$$

where ^{56}Fe is the projectile, ^{27}Al is the target, and X are the leftover projectile and target fragments. The mass number, A, and the atomic number, Z, must add up to 71 and 33, respectively.

3.1 Heavy Ion Nuclear Cross Sections

NUCFRG2 is a classical, geometric model based on the abrasion - ablation concept [21], whereby a piece of the incoming projectile nucleus is sheared off (abraded) by collision with the target. The abraded piece is formed in a highly excited state, which subsequently decays (ablates) by energetic particle emission. The model is geometric in the sense that the entire abrasion - ablation process is determined by considering the relative impact parameter of colliding spherical nuclei. NUCFRG2 neglects quantum mechanical effects and does not include important shell structure information. Therefore, one of its weaknesses is the inability to account for the odd - even effect observed in experimental data, where cross sections for fragments with an even number of nucleons are systematically larger than cross sections for fragments with an odd number of nucleons. This phenomenon is clearly related to the nuclear pairing interaction. Efforts are currently underway [22] to upgrade NUCFRG2 to include this effect, as well as to describe light ion production via coalescence.

3.2 Nucleon and Light Ion Nuclear Cross Sections

Total and differential energy cross sections for nucleon and light ion projectiles are handled outside of the NUCFRG2 model by a set of subroutines within OLTARIS (previously embedded

in HZETRN2005). Processes relevant to the nuclear interactions of nucleons and light ions are utilized and include elastic scattering, light ion knockout and pickup, light ion projectile fragmentation, and target fragmentation. The cross sections for these processes are largely modeled by empirical and semi-empirical parameterizations [4, 9, 23, 24, 25, 26, 27, 28, 29].

3.3 Atomic Cross Sections or Stopping Powers

The transport algorithms solve the Boltzmann equation using the continuous slowing down approximation (CDSA) with stopping powers and residual ranges calculated using Bethe theory with corrections [4, 30]. The transport solution uses scaled proton stopping power and ranges for all ions but directly calculates stopping power individually for each isotope when calculating some response functions.

4 Radiation Environment or Boundary Conditions

The radiation environments within OLTARIS are computed in a modular fashion, whereby for a given spacecraft flight condition, the input particle(s) spectrum on the external boundary of the spacecraft has to be defined to initiate the transport through bulk matter. The input boundaries can be Galactic Cosmic Rays (GCR) [31, 32], Solar Particle Events (SPE) [4, 33, 34, 35, 36], trapped protons within the Earth's geomagnetic field [37, 38], and albedo neutrons from the Earth's atmosphere [39, 40, 41]. An energy spectrum for the particle field(s) with individual or combinations of these spectra is generated following a pre-determined input and output format to make them compatible with the transport as described in Section 5. There is also a Lunar Surface boundary condition where directions that point toward the surface are set to zero. The following sections describe the possible boundary conditions.

4.1 Solar Particle Event Spectra

A solar particle event (SPE) is a large number of protons accelerated by the sun's magnetic field. The historical SPE events and their corresponding differential formulas used in OLTARIS include[1]:

February 1956 Webber, with 100 MV rigidity [33]:

$$\phi(E) = 1.0 \times 10^7 \left[\frac{E+m}{\sqrt{E(E+2m)}} \right] \exp \left[\frac{239.1 - \sqrt{E(E+2m)}}{100} \right]$$

[1] m is the mass of the proton and is approximately 938 MeV

February 1956 LaRC [4]:

$$\phi(E) = 6.0 \times 10^7 \exp\left(\frac{10-E}{25}\right) + 9.375 \times 10^5 \exp\left(\frac{100-E}{320}\right)$$

November 1960 [4]:

$$\phi(E) = 6.33 \times 10^8 \exp\left(\frac{10-E}{12}\right) + 4.88 \times 10^6 \exp\left(\frac{100-E}{80}\right)$$

August 1972 King [34]:

$$\phi(E) = 2.98 \times 10^8 \exp\left(\frac{30-E}{26.5}\right)$$

August 1972 LaRC [4]:

$$\phi(E) = 2.2 \times 10^7 \exp\left(\frac{100-E}{30}\right)$$

August 1989 [35]:

$$\phi(E) = \frac{8.652 \times 10^{10}}{59.261} \frac{E+m}{\sqrt{E(E+2m)}} \exp\left[\frac{-\sqrt{E(E+2m)}}{59.261}\right]$$

September 1989 [35]: [2]

$$\phi(E \leq 10\,\mathrm{MeV}) = 1.446 \times 10^8 \frac{E+m}{\sqrt{E(E+2m)}} \exp\left[\frac{-\sqrt{E(E+2m)}}{102.118}\right]$$

$$\phi(10\,\mathrm{MeV} < E < 30\,\mathrm{MeV}) = \left[-0.0015E^2 + 0.07184E + 0.4304\right] \phi(E \leq 10\,\mathrm{MeV})$$

$$\phi(E \geq 30\,\mathrm{MeV}) = \frac{2.034 \times 10^7}{\sqrt{1 - \left(\frac{m}{E+m}\right)^2}} \left[\sqrt{\frac{E(E+2m)}{30(30+2m)}}\right]^{-4.5}$$

[2] A smoothing function has been added in the 10 to 30 MeV range, and $\phi(E \leq 10\,\mathrm{MeV})$ in the smoothed equation is evaluated at the input energy range between 10 MeV and 30 MeV.

October 1989 [35]:

$$\phi(E) = 6.104 \times 10^8 \left[\frac{E+m}{\sqrt{E(E+2m)}}\right] \exp\left[\frac{-\sqrt{E(E+2m)}}{92.469}\right]$$

Carrington 1859, with 1989 fit [36]:

$$\phi(E) = 0.877 \times 0.3841 E^{0.3841-1} \times 4.79 \times 10^{11} \exp\left(-0.877 E^{0.3841}\right)$$

Carrington 1859, with 1991 fit [36]:

$$\phi(E) = 0.972 \times 0.441 E^{0.441-1} \times 1.47 \times 10^{12} \exp\left(-0.972 E^{0.441}\right)$$

LaRC stands for Langley Research Center. The boundary condition defines the units used in the rest of the OLTARIS processes. The units for all of the differential SPE spectra defined above are $\frac{\text{protons}}{\text{cm}^2-\text{AMeV}-\text{event}}$.

4.2 Galactic Cosmic Rays

The model developed by O'Neill [31] is used as GCR input for OLTARIS. This GCR model is based on fitting the existing balloon and satellite measured energy spectra from 1954 to 1992 and more recent measurements from the Advanced Composition Explorer satellite from 1997 to 2002 with the stationary Fokker-Planck equation. This fit solves the diffusion, convection, and energy loss boundary value problem and obtains an estimate of the appropriate diffusion coefficient. In addition, correlation of the diffusion coefficient with the Climax neutron monitor data, which exhibits an odd-even cycle with a 22 year period, enables the estimation of the diffusion coefficient at times when direct observational data are not available. The implementation of this GCR model accurately accounts for the solar modulation of hydrogen through nickel by propagating the Local Interplanetary Spectrum of each element through the heliosphere. The model provides a single value of the deceleration parameter $\phi(t)$ describing the level of solar cycle modulation and determines the GCR differential energy spectrum for elements from hydrogen to nickel at any given radial distance from the sun.

The earliest date available for input into the system is 01-Jan-1951. The latest date is variable and is controlled by the OLTARIS user interface. Please check the website for the latest date available. The user has three input methods:

1. Start and end dates from pull-down lists of the day, month, and year.
2. Start date from pull-down lists of the day, month, and year and the mission duration in days.
3. Preset scenarios with mission duration in days.

There are currently eleven preset scenarios available for user selections. Table 1 outlines the deceleration parameter for each of the scenarios. The boundary condition defines the units used in the rest of the OLTARIS processes. The units for the GCR environment are $\frac{\text{particles}}{\text{cm}^2-\text{AMeV}-\text{day}}$.

Table 1: Deceleration Parameters for Preset OLTARIS GCR Scenarios

Scenario	Deceleration Parameter
1956 Solar Min	401
1959 Solar Max	1986
1965 Solar Min	510
1970 Solar Max	1293
1977 Solar Min (DSNE[3])	474
1982 Solar Max	1924
1987 Solar Min	467
1991 Solar Max	2525
1997 Solar Min	467
2000 Solar Max	1674
2007 Solar Min (predicted)	490

[3]DSNE - Constellation Program Design Specification for Natural Environments [32].

4.3 Earth Orbit

The Earth Orbit (EO) boundary condition consists of three components: GCR, omni-directional trapped protons, and atmospheric albedo neutrons. There are several options for specifying an EO environment on OLTARIS. The user can input mission dates with altitude and inclination or select the DSNE environment (Constellation Program Design Specification for Natural Environments [32]), which will fix the dates, altitude, and inclination. The user can also select which of the three components are to be included.

4.3.1 Galactic Cosmic Rays

The GCR model of Section 4.2 is modulated by a direction averaged geomagnetic transmission coefficient scaled by global vertical cutoff data using the model in references [42, 43, 44] to produce charge and energy dependent differential spectra. The acceptable altitude range for input is 200 to 20,000 km. The units of this boundary condition are in $\frac{\text{particles}}{\text{cm}^2-\text{AMeV}-\text{day}}$.

4.3.2 Omni-directional Trapped Protons

The trapped proton model is calculated using AP8MIN and AP8MAX proton flux models based on the Vette reduction of satellite data [37, 38]. AP8MIN is interpolated on the Jenson and Cain

[45] geomagnetic field model and AP8MAX is interpolated on the Cain [46] geomagnetic field model extrapolated forward in time to 1970. As a side note, within the South Atlantic Anomaly region, the trapped proton field dips down to about 200 km, which is well within the orbits of the Space Transportation System (STS) or Shuttle and the International Space Station (ISS) missions. The acceptable altitude range for input is 200 to $20,000$ km. The units of the omni-directional trapped proton flux are $\frac{\text{particles}}{\text{cm}^2-\text{AMeV}-\text{day}}$.

4.3.3 Atmospheric Albedo Neutrons

Atmospheric albedo neutrons result from the interaction of GCR with the Earth's atmosphere. As the GCR intensities are modulated by solar activity so are the atmospheric neutrons modulated with time. The atmospheric neutron model [40] is a parametric fit to data gathered by NASA Langley Research Center's studies of the radiations at Supersonic Transport altitudes in the years 1965 to 1971. It covers the rise and decline of solar cycle 20. Scaling of the data, with respect to geomagnetic cutoff, altitude, and modulation of the Deep River Neutron Monitor, was found to allow for mapping of the environment to all locations at all times resulting in an empirically based model for the atmospheric albedo neutrons used in OLTARIS. The units of the atmospheric albedo neutrons flux are $\frac{\text{neutrons}}{\text{cm}^2-\text{AMeV}-\text{day}}$.

4.4 Lunar Surface

The lunar surface environment is currently implemented on OLTARIS in a simplified manner. The user can select either a lunar SPE or a lunar GCR environment. In each case, the corresponding free-space spectrum is computed and then applied to all of the rays in the vehicle thickness distribution not pointing toward the lunar surface. The surface pointing rays, which must be indicated in the thickness distribution, will have a *zero* boundary applied. At this time, a lunar neutron albedo spectrum has not been implemented, so this zero-contribution from the surface is an approximation. The lunar neutron albedo will be added as a future enhancement to OLTARIS.

5 Particle Transport

The particle transport module in OLTARIS is used to propagate particles of an ambient space radiation environment (See Section 4) through a combination of vehicle, shielding, and/or tissue. The transport algorithms in HZETRN2005 were developed by Wilson et al. [4, 9, 47] and Cucinotta [48]. Slaba et al. [17] have since modified the algorithms so that faster and more accurate methods are used. The bi-directional neutron transport algorithms used in the slab calculations were developed by Slaba et al. [16, 49]. In general, the transport algorithms provide an

approximate numerical solution to the linearized Boltzmann transport equation with the Continuous Slowing Down Approximation (CSDA) and the straight ahead approximation [4] to yield:

$$\left[\frac{\partial}{\partial x} - \frac{1}{\mathrm{A}_j}\frac{\partial}{\partial E}S_j(E) + \sigma_j(E)\right]\phi_j(x,E) = \sum_k \int_E^\infty \mathrm{d}E'\ \sigma_{k\to j}(E'\to E)\phi_k(x,E') \tag{1}$$

with the boundary condition

$$\phi_j(0,E) \ = \ f_j(E),$$

where $\phi_j(x,E)$ is the flux or fluence of type j particles at depth x with kinetic energy E. In equation 1, A_j is the atomic mass number of a type j particle, $S_j(E)$ is the stopping power of a type j ion with kinetic energy E, $\sigma_j(E)$ is the total macroscopic cross section for a type j particle with kinetic energy E, and $\sigma_{k\to j}(E' \to E)$ is the macroscopic production cross section for interactions in which a type k particle with kinetic energy E' produce a type j particle with kinetic energy E. The summation limits in equation 1 will be discussed shortly. The boundary condition spectrum, $f_j(E)$, is considered to be a known function over a broad energy spectrum and has been discussed in Section 4.

The left hand side is known as the Boltzmann operator, and the right hand side is the scattering kernel or collision operator. The Boltzmann operator in equation 1 consists of a streaming term in one dimension of space and no dimensions of angle, the CSDA term in energy, and the total interaction probability. The scattering kernel sums and integrates over all particles and energies to represent the source of secondary particles produced through fragmentation and elastic interactions.

The CSDA is based on the assumption that sufficiently many atomic interactions occur per unit path length to allow them to be expressed as a continuous process. The straight ahead approximation is based on the assumption that all primary and secondary particles propagate in the same direction. This reduces the transport equation to one spatial dimension and no angular dimensions. The particle source is the boundary condition; therefore, a marching algorithm can be used to solve the equations in the direction of interest.

Transport solutions for light ions ($\mathrm{A}\leq 4$) (including neutrons) and heavy ions ($\mathrm{A}>4$) are obtained separately, as demanded by the treatment of the nuclear cross sections and external space radiation environments. For heavy ions, it is known that prompt projectile fragments have a velocity, or energy per mass unit, very near that of the projectile (the constant velocity approximation), while de-excitation particles from the projectile fragments are produced nearly isotropically with lower energy [5]. The heavy ion projectile produced target fragments are neglected in the transport procedure due to their low energy and hence range. These approximations greatly simplify the transport equation (equation 1). If all transported heavy ions are ordered according to mass, then the heavy ion ($\mathrm{A}>4$ & $\mathrm{Z}>2$) transport equation can be succinctly written as

$$\left[\frac{\partial}{\partial x} - \frac{1}{\mathrm{A}_j}\frac{\partial}{\partial E}S_j(E) + \sigma_j(E)\right]\phi_j(x,E) = \sum_{k>j} \sigma_{k\to j}(E)\phi_k(x,E), \tag{2}$$

where $\sigma_{k\rightarrow j}(E)$ is the production cross section for interactions in which a type k particle with energy E produces a type j particle with energy E. The upper summation limit in equation 2 can vary, and OLTARIS currently uses 59 ions (See Table 2). For light particles, the equal velocity approximation is not valid and both the light projectile and the target fragments are included in the transport procedure. In this case, equation 1 is solved, and the summation is taken over all light particles: the lightest six particles in Table 2.

Table 2: OLTARIS Transported Isotopes

Isotope	A	Z	Isotope	A	Z	Isotope	A	Z
Neutron	1	0	^{1}H	1	1	^{2}H	2	1
^{3}H	3	1	^{3}He	3	2	^{4}He	4	2
^{6}Li	6	3	^{7}Li	7	3	^{8}Be	8	4
^{9}Be	9	4	^{10}B	10	5	^{11}B	11	5
^{12}C	12	6	^{13}C	13	6	^{14}N	14	7
^{15}N	15	7	^{16}O	16	8	^{17}O	17	8
^{18}F	18	9	^{19}F	19	9	^{20}Ne	20	10
^{21}Ne	21	10	^{22}Ne	22	10	^{23}Na	23	11
^{24}Mg	24	12	^{25}Mg	25	12	^{26}Mg	26	12
^{27}Al	27	13	^{28}Si	28	14	^{29}P	29	15
^{30}S	30	16	^{31}S	31	16	^{32}S	32	16
^{33}Cl	33	17	^{34}Ar	34	18	^{35}Cl	35	17
^{36}Ar	36	18	^{37}K	37	19	^{38}Ar	38	18
^{39}K	39	19	^{40}Ca	40	20	^{41}Ca	41	20
^{42}Ca	42	20	^{43}Sc	43	21	^{44}Ti	44	22
^{45}Ti	45	22	^{46}Ti	46	22	^{47}Ti	47	22
^{48}V	48	23	^{49}V	49	23	^{50}Cr	50	24
^{51}Cr	51	24	^{52}Cr	52	24	^{53}Mn	53	25
^{54}Mn	54	25	^{55}Fe	55	26	^{56}Fe	56	26
^{57}Co	57	27	^{58}Ni	58	28			

The light ion and heavy ion transport solution methodology is expressed in marching algorithms and have been analytically shown to be accurate to $O(h^2)$ where h is the step-size in units of $\frac{\text{g}}{\text{cm}^2}$ [4]. Slaba et al. [14, 17] have also controlled the energy discretization error through various modifications to the light ion transport algorithm. An extensive review of the verification and validation efforts associated with the HZETRN2005 marching algorithms can be found in Wilson et al. [5]. A detailed derivation of the marching algorithms including the recent updates, can be found in Slaba et al. [17].

In the current OLTARIS implementation, two transport scenarios are used:

1. Three material layer database for interpolation currently set to aluminum, polyethylene, and tissue.

2. Multiple layer slab with coupled bi-directional neutron transport.

Item 1 generates a database of every combination of the three materials from $0.05\frac{\text{g}}{\text{cm}^2}$ for SPE and EO and $0.1\frac{\text{g}}{\text{cm}^2}$ for GCR to at least $100\frac{\text{g}}{\text{cm}^2}$ with a spatial grid created to ensure spatial convergence of the thickness interpolation algorithms. If rays in the vehicle thickness file are larger than $100\frac{\text{g}}{\text{cm}^2}$, the grid is increased in increments of $50\frac{\text{g}}{\text{cm}^2}$ to cover the longest ray up to $1000\frac{\text{g}}{\text{cm}^2}$. The slab solution, item 2, allows the user to create materials and layer them so that a response function can be generated at the end of the slab and at each user defined thickness. The slab solution also utilizes a backward solution for neutrons [49]. Reference [17] has a full discussion of the coupled spatial step and energy grid size convergence criterion.

6 Response Functions

Once a flux or fluence spectrum as a function of particles and energies is calculated from the Boltzmann equation, equation 1, then that flux has to be modified to represent the response wanted by the user. Currently, OLTARIS determines dose (D), dose equivalent (H), thermoluminescence detector (TLD) response, Linear Energy Transfer (LET), Tissue Equivalent Proportional Counter (TPEC) response, and effective whole body dose equivalent (ED). The TEPC and ED are only calculated for the interpolation transport scheme, but all others are calculated for the slab and interpolation schemes as explained in Section 5. Therefore, D, H, TLD, and LET are determined at each of the interpolation edit points and are interpolated over a thickness file described in Section 2.2 to get the values at a point inside a geometry. For the slab, no interpolation is performed and the values are output at the slab boundary points input by the user. The TEPC and ED calculations are more complex and need a vehicle description to become meaningful. Each of these responses is discussed in detail below.

6.1 Dose

While the flux of particles is a detailed quantity describing the environment inside a spacecraft, it is of little use to inform the user about the damage caused by or the risk resulting from this particle environment to humans, materials, or electronics. As a first step, the dose is calculated from the energy deposited along every particle's track as it traverses the spacecraft. Therefore, the dose is defined as

$$D = \sum_j D_j,$$

where,

$$D_j = \int_0^\infty dE\ S_j(E)\phi_j(E) + d^\star(E)$$

with $S_j(E)$ as the stopping power of a charged particle j at energy E in the material of interest (usually tissue or silicon) in units of $\frac{\text{keV}}{\mu\text{m}}$. Of course, the stopping power of neutral particles in any material is zero; therefore, the integral term is zero. Since heavy target fragments and recoil nuclei are not transported, their dose is added by the $d^\star(E)$ function [50]. The units of Dose are mGy. Dose can be reported in tissue or silicon.

The dose is calculated at all interpolation grid points or slab points. This is called the Dose Table or Dose versus Depth Table. This table can be interpolated over a set of thickness files to obtain a dose at a point inside a vehicle and/or human.

6.2 Dose Equivalent

While dose gives the energy deposited by a particle in a material, it does not estimate the probability of stochastic effects in humans such as cancer mortality. For the "complex mixture of high- and low-LET radiation experienced in LEO," [51] the National Council on Radiation Protection and Measurement (NCRP) endorses the use of dose equivalent calculated with the ICRP-60 [52] quality factor, $Q_{\text{ICRP}-60}$, for this purpose [51, 53, 54]. As yet, the NCRP has not made a recommendation for space environments beyond LEO [54], but NASA has adopted the approach of using dose equivalent for beyond LEO vehicles as well. Dose Equivalent is defined as

$$H = \sum_j H_j,$$

where,

$$H_j = \int_0^\infty dE\; Q_{\text{ICRP}-60}\left(S_j(E)\right) S_j(E)\phi_j(E) + h^\star(E).$$

The quality factor $Q_{\text{ICRP}-60}$ is defined as [52]

$$Q_{\text{ICRP}-60}\left(S_j(E)\right) = \begin{cases} 1 & \text{for} \quad 0 < S_j(E) \leq 10 \\ 0.32S_j(E) - 2.2 & \text{for} \quad 10 < S_j(E) \leq 100 \\ \frac{300}{\sqrt{S_j(E)}} & \text{for} \quad 100 > S_j(E) \end{cases},$$

where $S_j(E)$ is the stopping power of a charged particle j at energy E in the material, tissue, or organ of interest in units of $\frac{\text{keV}}{\mu\text{m}}$. The stopping power of neutral particles in any materials is zero; therefore, the integral term is zero. Since heavy target fragments and recoil nuclei are not transported, their dose equivalent is added by the $h^\star(E)$ function [50]. The units of Dose Equivalent are mSv.

The dose equivalent is calculated at all interpolation grid points or slab points. This is called the Dose Equivalent Table or Dose Equivalent versus Depth Table. This table can be interpolated over a set of thickness files to obtain a dose equivalent value at a point inside a vehicle and/or human.

6.3 TLD-100

For dosimetry measurement purposes, one of the most widely used phosphor based instruments is the Lithium-Fluoride thermo-luminescence detector (TLD-100). These instruments are routinely flown on ISS and STS missions and were used for validation of OLTARIS. Within OLTARIS, the flux response function for the TLD-100 sensitivity to an incoming ion of charge Z and energy E is modeled by the functional fit [55]

$$F_{\mathrm{TLD}}(E,Z) = 0.2418 + 0.8205 \exp\left\{-0.002\left[\frac{y(Z)}{\gamma(E)}\right]^2\right\},$$

where

$$y(Z) = Z\left\{1 - \exp\left[-125\left(\frac{\gamma(E)}{Z}\right)^{\frac{2}{3}}\right]\right\},$$

and

$$\gamma(E) = \sqrt{1 - \frac{1}{\left(1 + \frac{E}{932}\right)^2}}.$$

The non-dimensional quantity $F_{\mathrm{TLD}}(E,Z)$ then scales the appropriate flux values at a given depth, energy, and charge. Finally, the scaled fluxes are integrated over energy and summed over charge to get the TLD-100 response to the particle field.

The TLD-100 response is calculated at all interpolation grid points or slab points. This is called the TLD-100 Table or TLD-100 versus Depth Table. This table can be interpolated over a set of thickness files to obtain a TLD-100 value at a point inside a vehicle and/or human.

6.4 Integral and Differential Linear Energy Transfer (LET)

In analyzing charged particle spectra in space due to GCR, SPE, and trapped protons, the conversion or mapping of particle energy spectra into LET distributions is a convenient guide in assessing biologically significant components of these spectra. The mapping of LET to energy is a triple valued function and can be defined only on open energy subintervals where the derivative of LET with respect to energy is not zero. OLTARIS uses a well-defined numerical procedure, which allows for the generation of LET spectra on the open energy subintervals that are integrable in spite of their singular nature [56, 57]. LET can be reported in tissue and silicon.

The differential and integral LET distributions are calculated at all interpolation grid points or slab points. These are called the LET Distributions or LET versus Depth Distributions. These distributions can be interpolated over a set of thickness files to obtain a differential and integral LET distribution at a point inside a vehicle and/or human.

The units of differential LET based flux are $\frac{\mathrm{particles}}{\mathrm{cm}^2 \frac{\mathrm{keV}}{\mu\mathrm{m}} \mathrm{day-or-event}}$. The units of integral or cumulative LET based flux are $\frac{\mathrm{particles}}{\mathrm{cm}^2-\mathrm{day-or-event}}$. LET has units of $\frac{\mathrm{keV}}{\mu\mathrm{m}}$.

6.5 Tissue Equivalent Proportional Counter (TEPC)

In contrast to the limitations of LET based passive detectors, TEPC detectors simulate a micron-sized tissue site and can provide a time resolved spectra in lineal energy. While the mapping of flux/fluence into LET is a convenient guide in assessing biologically significant components of these spectra, a feature of ionizing radiation is that it has a discontinuous nature in interacting with matter. The deposited energy into a medium consists of discrete events with energy partitioning among ionization and excitation processes. This observation led to the suggestion that the usual LET dependent quality factor (Q) be replaced by a lineal energy dependent Q for use in radiation protection studies. Furthermore, the usual method of measuring LET is based on passive plastic track detectors with limited LET range. These detectors can not detect electrons, their efficiency for detection of secondaries, such as pions or kaons, are not well established, and they experience detection-resolution limitation above an LET of approximately 250 to $300\frac{\mathrm{keV}}{\mu\mathrm{m}}$. Finally, because of the passive nature of these detectors, the separation of GCR from trapped particles for LEO flights is difficult.

Monte Carlo (MC) simulations are the method of choice to model energy deposition by ions in a micro-volume. MC necessitates a complete model of the important components of the TEPC device and depending on the uncertainty wanted, can take some time to execute. In contrast, OLTARIS uses a computationally efficient deterministic method for the numerical representation of stochastic energy deposition and ionization produced by energetic ions passing through absorber sites of submicron dimension [58, 59]. The Xapsos methodology and its extension to obtain the response of a TEPC is an attempt to provide an accurate prediction for comparison with spacecraft measurements [57].

The units of lineal energy are $\frac{\mathrm{keV}}{\mu\mathrm{m}}$. The units of differential TEPC response flux/fluence are $\frac{\mathrm{particles}}{\mathrm{cm}^2\mathrm{sr}\frac{\mathrm{keV}}{\mu\mathrm{m}}\mathrm{day-or-event}}$. The units of integral TEPC response flux/fluence are $\frac{\mathrm{particles}}{\mathrm{cm}^2\mathrm{sr\,day-or-event}}$.

6.6 Effective and Organ Averaged Dose Equivalent

As is recommended in NCRP-132 and NCRP-142 [51, 53], effective dose equivalent is calculated by first calculating the averaged dose equivalent for the organs and tissues listed in Table 3. The remainder organs are listed in NCRP-132 as: adrenals, brain, small intestine, large intestine, kidneys, muscle, pancreas, spleen, thymus, and uterus. A weighted average of these organ or tissue dose equivalent values, as defined in equation 3, is then calculated using the NCRP-132 tissue weighting factors given in Table 3.

$$ED = \sum_{T} w_T \bar{H}_T, \tag{3}$$

where w_T are the NCRP-132 tissue weighting factors in Table 3 and $\bar{H}_T$ are the organ or tissue averaged dose equivalents as calculated by OLTARIS.

Organ or tissue averaged dose equivalent is calculated by first calculating the dose equivalent at a large enough number of target points in the organ or tissue to accurately characterize that

Table 3: NCRP 132 Organs and their weights

Tissue Weights	0.01	0.05	0.12	0.20
Tissue Types	Bone Surface Skin	Bladder Breast Liver Esophagus Thyroid Remainder	Bone Marrow Colon Lung Stomach	Gonads

organ or tissue and then averaging these point values. Currently, the user can select one of four human body models (CAM [60], CAF [61, 62], MAX [63], or FAX [64]) for these calculations. Target point locations for all of the necessary organs and tissues in each of the human body models have been chosen [15, 65], and body thickness distributions are combined with vehicle thickness distributions as described in Section 2.2.

There are a few body model specific details that should be noted. First, there are ten remainder organs for the females, but only nine for the males. For this reason, the tissue weighting factor, w_T, for each of the remainder organs is $\frac{0.05}{10}$ for females and $\frac{0.05}{9}$ for the males. Second, in the CAF and CAM models, the colon, large intestine, and small intestine are treated as one organ. This organ labeled intestine is therefore assigned a tissue weighting factor equivalent to the sum of the tissue weighting factor specified for the colon, 0.12, and the tissue weighting factors for two remainder organs. Thus, the intestine weighting factor is $0.12 + \frac{0.05}{10} \times 2$ for CAF and $0.12 + \frac{0.05}{9} \times 2$ for CAM. Similarly, the colon and the large intestine are treated as one organ and labeled "colon" in the FAX and MAX models, but the small intestine is treated as a separate organ in these models. The weighting factor for the colon is therefore $0.12 + \frac{0.05}{10}$ in FAX and $0.12 + \frac{0.05}{9}$ in MAX. Also, the organ averaged dose equivalent is calculated for several organs not included in the effective dose equivalent calculation. These organs are heart, hippocampus, lens, and salivary glands for the CAF model; heart, hippocampus, lens, prostate, and salivary glands for the CAM model; heart, hippocampus, lens, retina, salivary glands, and trachea for the FAX model; and heart, hippocampus, lens, prostate, retina, salivary glands, and trachea for the MAX model.

7 Summary and Future Work

The OLTARIS website is a versatile tool in the analysis of vehicles for human space flight that enables the designers to meet NASA's requirements for space radiation protection throughout all stages of vehicle design. The tools within OLTARIS are securely managed, have undergone a rigorous verification and validation process, and are presented to the user in an easy to follow

format. This is achieved with modern tools, a modern understanding of how user's operate, and with many people thinking through this problem to get a solution that best fits the tools available and the user needs. Tools are available for the materials and spacecraft design community on the OLTARIS website. A user can define their own material and transport any available space environment through it or through multiple slabs of any reasonable number and thickness. An example use case is described in the Appendix. This paper has also discussed material properties, Earth orbit, particle transport and response functions.

OLTARIS can be easily modified to accommodate new user needs and wants. Adding new features is straightforward because of the nature of the web interface. Adding new calculations is also straightforward due to the modularity of the computational engine behind the website. The connection of the website interface to the analysis modules with the Sun Grid Engine allows external sites to be incorporated, with appropriate security issues resolved, to execute new models without giving control of those calculations to the OLTARIS team. Interface file formats are clearly defined and can be used to connect new parts with old parts to create new calculations. All of these functions are connected through use cases.

For the near future, use cases will be generated for electronic response functions either within OLTARIS or in conjunction with other sites and new transport algorithms. The near term transport algorithm addition will be a ray-by-ray transport where the transport algorithm is executed along each ray in the spacecraft's thickness file. Each ray will have a complete slab based transport calculation performed. The results for each ray will then be integrated together to obtain the response wanted by the user.

Longer term projects could include Monte Carlo solutions for multi-layer slab geometries, more user control of the existing transport algorithms, new tracked particles in the marching algorithm like electrons and pions, user specified materials in the interpolation transport algorithm, five or more material layer interpolation transport algorithm, and better and more accurate interaction cross sections to replace NUCFRG2. Of course, as this tool becomes more mature and gains users, the users will drive future improvements and priorities.

This project develops and maintains an integrated tool set (through the OLTARIS website) that collects the current best practices, databases, and state-of-the-art methodologies to evaluate and optimize space radiation protection for human systems such as spacecraft, spacesuits, rovers, and habitats. The modular nature of this development allows for easy verification and validation of methods employed as well as the ability to provide quick access to improvements in physics and transport for the radiation community under a configuration managed environment. This tool will increase fidelity by incorporating common spacecraft and user specified materials into the geometry description with the soon-to-be implemented ray-by-ray transport algorithm to further minimize uncertainties due to range-scaling of material thicknesses and material ordering. The ray-by-ray algorithm specifically addresses the limitations associated with simplified geometry description (equivalent aluminum, three-layer transport interpolation, random astronaut orientation) and straight ahead transport. The ray-by-ray algorithm will also establish the basis to calculate the forward/backward neutron transport for vehicle and lunar surface geometries. The back-scattered neutron environment will be calculated from the opposite

sides of the vehicle for a crew member's specific orientation at specific tissue locations. This will increase NASA's ability to evaluate the effectiveness of shielding systems.

A Example Use Case

This appendix shows an example use case used to help generate the OLTARIS user interface. The use case is broken up into sections that show a full description of the job, the job flow, any alternatives, and status.

UC-P02: Effective Whole-body Dose Equivalent Calculation with oriented astronaut

Summary: Effective dose is a response calculation that requires dose equivalent evaluations at multiple points throughout the body. Usually, approximations are made to assume a random orientation of the astronaut within the vehicle. However, it is desired to have the capability to orient an astronaut at a specific location in the vehicle. This use case describes a technique that utilizes a CAD-geometry phantom astronaut that is used to locate and orient the astronaut in the users vehicle CAD geometry. This type of calculation is typically used for short-duration events such as an SPE.

Preconditions: User has account and is logged in.

Direct Actors: All users

Triggers: User creates new project

Main Success Scenario:

1. User inputs a descriptive title of their choosing that will be used to reference the project
2. User adds a sentence or paragraph giving more details on the project
3. User selects an historic SPE with desired multiplication factor
4. User selects "phantom astronaut" for geometry setup
5. User downloads phantom CAD geometry in desired format (IGES, obj, ...)
6. User saves project and possibly logs out of design tool while orienting phantom in vehicle geometry
7. User opens project and uploads phantom "reference points" coordinates to the design tool in the vehicle coordinate system
8. User downloads properly oriented ray distribution from design tool
9. User raytraces vehicle at "phantom zone points" using download ray distribution

10. User uploads vehicle raytrace
11. User selects desired responses including effective dose
12. User submits job
13. User examines results in the form of numbers, tables, and plots as appropriate

Alternative Scenario Extensions:

- If an error condition results, the user is notified
- User can select different phantoms based on number of zones. More zones increase the accuracy of the calculation with respect to geometry, but requires more ray-tracing of the vehicle geometry. In the limit, the user could ray-trace all body points used in effective dose calculation

Post Conditions: Project is successfully run and returns results to user

Notes and Questions: None

End State: Finished

Once the use case is defined, then Fortran code, perl scripts, data files and whatever else is needed is assembled in an input, output, and process flowchart. The resultant system is then module tested and placed in the functional test stream. Ruby scripts that tie the process together are then generated, and the webpages are modified to incorporate use case into OLTARIS.

References

[1] NASA, "NASA Standards for Modeling and Simulation," NASA-STD-7009.

[2] Blattnig, S.R., Luckring, J.M., Morrison, J.H., Sylvester, A.J., Tripathi, R.K., Zang, T.A., "NASA Standard for Models and Simulations: Philosophy and Requirements Overview," AIAA-2009-1010, 47th AIAA Aerospace Sciences Meeting including The New Horizons Forum and Aerospace Exposition, Orlando, Florida, Jan. 5-8, 2009.

[3] Singleterry, R.C., Wilson, J.W., Shinn, J.L., Tripathi, R.K., Thibeault, S.A., Noor, A.K., Cucinotta, F.A., Badavi, F.F., Chang, C.K., Qualls, G., Clowdsley, M.S., Kim, M.Y., Heinbockel, J.H., Norbury, J.W., Blattnig, S.R., Miller, J., Zeitlin, C., Heilbronn, L.H., "Creation and Utilization of a World Wide Web Based Space Radiation Effects Code: SIREST," Physica Medica, Vol. XVII, suppl. 1, p. 90, 2001.

[4] Wilson, J.W., Townsend, L.W., Schimmerling, W., Khandelwal, G.S., Khan, F., Nealy, J.E., Cucinotta, F.A., Simonsen, L.C., Shinn, J.L., Norbury, J.W., "Transport Methods and Interactions for Space Radiations," NASA Reference Publication 1257, 1991.

[5] Wilson, J.W., Tripathi, R.K., Mertens, C.J., Blattnig, S.R., Clowdsley, M.S., Cucinotta, F.A., Tweed, J., Heinbockel, J.H., Walker, S.A., Nealy, J.E., "Verification and Validation: High Charge and Energy (HZE) Transport Codes and Future Development," NASA Technical Paper 213784, 2005.

[6] Wilson, J.W., Tripathi, R., Cucinotta, F., Shinn, J., Badavi, F., Chun, S., Norbury, J.W., Zeitlin, C.J., Heilbronn, L., Miller, J., "NUCFRG2: An Evaluation of the Semi-empirical Nuclear Fragmentation Database," NASA Technical Paper 3533, 1995.

[7] Wilson, J.W., Townsend, L.W., Badavi, F.F., "A Semi-empirical Nuclear Fragmentation Model," Nuclear Instruments and Methods in Physics Research B, Vol. 18, pp. 225-231, 1987.

[8] Wilson, J.W., Shinn, J.L., Townsend, L.W., Tripathi, R.K., Badavi, F.F., Chun, S.Y., "NUCFRG2: a Semi-empirical Nuclear Fragmentation Model," Nuclear Instruments and Methods in Physics Research B, Vol. 18, pp. 95-102, 1994.

[9] Wilson, J.W., Townsend, L.W., Nealy, J.E., Chun, S.Y., Hong, B.S., Buck, W.W., Lamkin, S.L., Ganapol, B.D., Khan, F., Cucinotta, F.A., "BRYNTRN: A Baryon Transport Model," NASA Technical Paper 2887, 1989.

[10] http://rubyonrails.org/, accessed 03-March-2010.

[11] http://www.mysql.com/, accessed 03-March-2010.

[12] http://httpd.apache.org/, accessed 03-March-2010.

[13] http://gridengine.sunsource.net/, accessed 03-March-2010.

[14] Slaba, T.C., Blattnig, S.R., Clowdsley, M.S., Walker, S.A., Badavi, F.F., "An Improved Neutron Transport Algorithm for HZETRN2005," NASA Technical Paper 216199, 2010.

[15] Slaba, T.C., Qualls, G.D., Clowdsley, M.S., Blattnig, S.R., Simonsen, L.C., Walker, S.A., Singleterry, R.C., "Analysis of Mass Averaged Tissue Doses in CAM, CAF, MAX, and FAX", NASA Technical Paper 215562, 2009.

[16] Slaba, T.C., Heinbockel, J.H., Blattnig, S.R., "Neutron Transport Models and Methods for HZETRN and coupling to Low Energy Light Ion Transport," SAE International Journal of Aerospace, Vol. 1, No. 1, pp. 510-521, 2009

[17] Slaba, T.C., Blattnig, S.R., Badavi, F.F., "Faster and More Accurate Transport Procedures for HZETRN," NASA Technical Paper 2010-216213, 2010.

[18] Heinbockel, J.H., Slaba, T.C., Blattnig, S.R., Tripathi, R.K., Townsend, L.W., Handler, T., Gabriel, T.A., Pinsky, L.S., Reddell, B., Clowdsley, M.S., Singleterry, R.C., Norbury, J.W., Badavi, F.F., Aghara, S.K., "Comparison of the Radiation Transport Codes HZETRN, HETC-HEDS and FLUKA using the February 1956 Webber SPE spectrum," NASA Technical Paper 2009-215560, 2009.

[19] Heinbockel, J.H., Slaba, T.C., Badavi, F.F., Blattnig, S.R., Norbury, J.W., Townsend, L.W., Handler, T., Gabriel, T.A., Pinsky, L.S., Reddell, B., Aumann, A.R., "A Comparison of the Radiation Transport Codes HZETRN, HETC-HEDS and FLUKA using the 1977 Solar Minimum GCR Spectrum," NASA Technical Paper 2009-215956, 2009.

[20] http://www.pmddtc.state.gov/regulations_laws/itar_official.html, accessed 03-March-2010.

[21] Hufner, J., Schafer, K., Schurmann, B., "Heavy Fragments Produced in Proton-nucleus and Nucleus-nucleus Collisions at Relativistic Energies," Physical Review C, Vol. 12, pp. 1888-1898, 1975.

[22] Norman, R., Blattnig, S., Norbury, J., "Nuclear Fragmentation Model Evaluation," Meeting of the Southeastern Section of the American Physical Society, Raleigh, North Carolina, October, 2008.

[23] Wilson, J.W., Townsend, L.W., Buck, W.W., Chun, S.Y., Hong, B.S., Lamkin, S.L., "Nucleon-Nucleus Interaction Data Base: Total Nuclear and Absorption Cross Sections," NASA Technical Memorandum 4053, 1988.

[24] Cucinotta, F.A., Townsend, L.W., Wilson, J.W., "Description of Alpha-nucleus Interaction Cross Sections for Cosmic Ray Shielding Studies," NASA Technical Paper 3285, 1993.

[25] Cucinotta F.A., "Calculations of Cosmic-Ray Helium Transport in Shielding Materials," NASA Technical Paper 3354, 1993.

[26] Cucinotta, F.A., Townsend, L.W., Wilson, J.W., Shinn, J.L., Badhwar, G.D., Dubey, R.R., "Light Ion Components of the Galactic Cosmic Rays: Nuclear Interactions and Transport Theory," Advances in Space Research, Vol. 17, pp. 77-86, 1996.

[27] Tripathi, R.K., Wilson, J.W., Cucinotta, F.A., "New Parameterization of Neutron Absorption Cross Sections," NASA Technical Paper 3354, 1997.

[28] Tripathi, R.K., Cucinotta, F.A., Wilson, J.W., "Universal Parameterization of Absorption Cross Sections," NASA Technical Paper 209726, 1999.

[29] Norbury, J.W., "Nucleon-Nucleon Total Cross Section," NASA Technical Paper 215116, 2008.

[30] Tai, H., Bichsel, H., Wilson, J.W., Shinn, J.L., Cucinotta, F.A., Badavi, F.F., "Comparison of Stopping Power and Range Databases for Radiation Transport Study," NASA Technical Paper 3644, 1997.

[31] O'Neill, P.M., "Badhwar-O'Neill Galactic Cosmic Ray Model Update Based on Advanced Composition Explorer (ACE) Energy Spectra from 1977 to Present," Advances in Space Research, Vol. 37, pp. 1727-1733, 2006.

[32] NASA, Constellation Program Design Specification for Natural Environments (DSNE), CxP 70023, Rev A, Change 001, Nov. 7, 2008.

[33] Webber, W.R., "An Evaluation of the Radiation Hazard due to Solar-Particle Events," D2-90469 Aero-Space Div., Boeing Co., 1963.

[34] King, J.H., "Solar Proton Fluences for 1977 - 1983 Space Missions," Journal of Spacecraft and Rockets, Vol. 11, No. 6, pp. 401-408, 1974.

[35] Sauer, H.H., Zwickl, R.D., Ness, M.J., "Summary Data for the Solar Energetic Particle Events of August Through December 1989," Space Environment Laboratory, National Oceanic and Atmospheric Administration, 1990.

[36] Townsend, L.W., Zapp, E.N., Stephens, D.L., Hoff, J.L., "Carrington Flare of 1859 as a Prototypical Worst-Case Solar Energetic Particle Event," IEEE Transactions on Nuclear Science, Vol. 50, No. 6, Dec. 2003.

[37] D. M. Sawyer, J. I. Vette, J.I., "AP-8 Trapped Proton Environments for Solar Maximum and Solar Minimum," NSSDC/WDC-A-R&S, pp. 76-06, 1976.

[38] Vette, J.I., "The NASA/National Space Science Data Center Trapped Radiation Environmental Model Program (1964-1991)," NSSDC/WDC-A-R&S, pp. 91-29, 1991.

[39] Foelsche, T., Mendell, R. B., Wilson, J. W., Adams, R. R., "Measured and Calculated Neutron Spectra and Dose Equivalent Rates at High Altitudes, Relevance to SST Operations and Space Research," NASA Technical Note D-7715, 1974.

[40] Wilson, J.W., *et al.*, "Cosmic Ray Neutron Albedo Dose in Low Earth Orbit," Health Physics, Vol. 57, pp. 665-668, 1989.

[41] Wilson, J.W., Denn, F. M., "Preliminary Analysis of the Implications of Natural Radiations on Geostationary Operations," NASA Technical Note D-8290, 1976.

[42] De Angelis, G., Clem, J.M., Goldhagen, P.E., Wilson, J.W., "A New Dynamical Atmospheric Ionizing Radiation (AIR) Model for Epidemiological Studies," Advances in Space Research, Vol. 32(1), pp. 17-26, 2003.

[43] Clem, J.M., De Angelis, G., Goldhagen, P., Wilson, J.W., "Preliminary Validation of Computational Procedures for a New Atmospheric Ionizing Radiation (AIR) Model," Advances in Space Research, 32(1), pp. 27-33, 2003.

[44] Wilson, J.W., Cucinotta, F.A., Golightly, M.J., Nealy, J.E., Qualls, G.D., Badavi, F.F., De Angelis, G., Anderson, B.M., Clowdsley, M.S., Luetke, N. Zapp, N., Shavers, M.R., Semones, E., Hunter, A., "International Space Station: A Test Bed for Experimental and Computational Dosimetry," Advances in Space Research, Vol. 37, pp. 1656-1663, 2006.

[45] Jensen, D.C., *et al.*, "An Interim Geomagnetic Field," Journal of Geophysical Research, No. 67, pp. 3568-3569, 1962.

[46] Cain, J.C., Hendricks, S.J., Langel, R.A., Hudson, W.V., "A Proposed Model for the International Geomagnetic Reference Field-1965," Journal of Geomagnetism and Geoelectricity, Vol. 19, pp. 335-355, 1967.

[47] Wilson, J.W., Badavi, F.F., "Methods of Galactic Heavy Ion Transport," Radiation Research, Vol. 108, pp. 231-237, 1986.

[48] Cucinotta, F.A., "Calculations of Cosmic-Ray Helium Transport in Shielding Materials," NASA Technical Paper 3354, 1993.

[49] Slaba, T.C., Blattnig, S.R., Aghara, S.K., "Coupled Neutron Transport for HZETRN," Radiation Measurements, in press, 2010.

[50] Personal Communication with John W. Wilson at the NASA Langley Research Center.

[51] National Council on Radiation Protection and Measurements (NCRP), "Operational Radiation Safety Program for Astronauts in Low-Earth Orbit: A Basic Framework," NCRP Report 142, 2002.

[52] International Commission on Radiological Protection (ICRP), "The 1990 Recommendations of the International Commission on Radiological Protection," ICRP Publication 60, Elsevier, New York, 1993.

[53] National Council on Radiation Protection and Measurements (NCRP), "Radiation Protection Guidance for Activities in Low-Earth Orbit," NCRP Report 132, 2000.

[54] National Council on Radiation Protection and Measurements (NCRP), "Information Needed to Make Radiation Protection Recommendations for Space Missions Beyond Low Earth Orbit," NCRP Report 153, 2006.

[55] Wilson, J.W., Tripathi, R.K., Badavi, F.F., Cucinotta, F.A., "Standardized Radiation Shield Design Method: 2005 HZETRN," International Conference on Environmental Systems (ICES), Norfolk, VA, No. 2006-01-2109, 2006.

[56] Badavi, F.F., Wilson, J.W., Hunter, A., "Numerical Study of the Generation of Linear Energy Transfer Spectra for Space Radiation Applications," NASA Technical Paper 213941, 2005.

[57] Badavi, F.F., Stewart-Sloan, C.R., Adams, D.O., Wilson, J.W., "Radiation Protection Effectiveness of Polymeric Based Shielding Materials at Low Earth Orbit," The Society for the Advancement of Material and Process Engineering (SAMPE), No. 2008-L002, May 2008.

[58] Xapsos, M.A., Burke, E.A., Shapiro, P., Summers, G.P., "Energy Deposition and Ionization Fluctuations Induced by Ions in Small Sites: An Analytical Approach," Radiation Research, Vol. 137, pp. 152-161, 1994.

[59] Xapsos, M.A, Burke, E.A., Shapiro, P., Summers, G.P., "Probability Distributions of Energy Deposition and Ionization in Sub-micrometer Sites for Condensed Media," Radiation Measurements, Vol. 26, pp. 1-9, 1996.

[60] Billings, M.P., Yucker, W.R., "The Computerized Anatomical Man (CAM) Model," Summary Final Report, MDC-G4655, McDonnell Douglas Company, 1973.

[61] Yucker, W.R., Huston, S.L., "The Computerized Anatomical Female," Final Report MDC-6107, McDonnell Douglas Company, 1990.

[62] Yucker, W.R., Reck, R.J., "Computerized Anatomical Female Body Self-Shielding Distributions," Report, MDC-92H0749, McDonnell Douglas Company, 1992.

[63] Kramer, R., Vieira, J.W., Khoury, H.J., Lima, F.R.A., Fuelle, D., "All about MAX: A Male Adult Voxel Phantom for Monte Carlo Calculations in Radiation Protection Dosimetry," Physics in Medicine and Biology, Vol. 48, pp. 1239-1262, 2003.

[64] Kramer, R., Vieira, J.W., Khoury, H.J., Lima, F.R.A., Loureiro, E.C.M., Lima, V.J.M., Hoff, G., "All about FAX: A Female Adult Voxel Phantom for Monte Carlo Calculations in Radiation Protection Dosimetry," Physics in Medicine and Biology, Vol. 49, pp. 5203-5216, 2004.

[65] Slaba, T.C., Qualls, G.D., Clowdsley, M.S., Blattnig, S.R., Walker, S.A., Simonsen, L.C., "Utilization of CMA, CAF, MAX, and FAX for Space Radiation Analysis Using HZETRN," Advances in Space Research, Vol. 45, pp. 866-883, 2010.

REPORT DOCUMENTATION PAGE

Form Approved
OMB No. 0704-0188

1. REPORT DATE *(DD-MM-YYYY)*	2. REPORT TYPE	3. DATES COVERED *(From - To)*
01- 07 - 2010	Technical Publication	

4. TITLE AND SUBTITLE
OLTARIS: On-Line Tool for the Assessment of Radiation in Space

5a. CONTRACT NUMBER

5b. GRANT NUMBER

5c. PROGRAM ELEMENT NUMBER

6. AUTHOR(S)
Singleterry, Robert C., Jr.; Blattnig, Steve R.; Clowdsley, Martha S.; Qualls, Garry D.; Sandridge, Christopher A.; Simonsen, Lisa C.; Norbury, John W.; Slaba, Tony C.; Walker, Steven A.; Badavi, Francis F.; Spangler, Jan L.; Aumann, Aric R.; Zapp, E. Neal; Rutledge, Robert D.; Lee, Kerry T.; Norman, Ryan B.

5d. PROJECT NUMBER

5e. TASK NUMBER

5f. WORK UNIT NUMBER
651549.02.07.01

7. PERFORMING ORGANIZATION NAME(S) AND ADDRESS(ES)
NASA Langley Research Center
Hampton, VA 23681-2199

8. PERFORMING ORGANIZATION REPORT NUMBER
L-19879

9. SPONSORING/MONITORING AGENCY NAME(S) AND ADDRESS(ES)
National Aeronautics and Space Administration
Washington, DC 20546-0001

10. SPONSOR/MONITOR'S ACRONYM(S)
NASA

11. SPONSOR/MONITOR'S REPORT NUMBER(S)
NASA/TP-2010-216722

12. DISTRIBUTION/AVAILABILITY STATEMENT
Unclassified - Unlimited
Subject Category 93
Availability: NASA CASI (443) 757-5802

13. SUPPLEMENTARY NOTES

14. ABSTRACT

The On-Line Tool for the Assessment of Radiation In Space (OLTARIS) is a World Wide Web based tool that assesses the effects of space radiation on humans and electronics in items such as spacecraft, habitats, rovers, and spacesuits. This document explains the basis behind the interface and framework used to input the data, perform the assessment, and output the results to the user as well as the physics, engineering, and computer science used to develop OLTARIS. The transport and physics is based on the HZETRN and NUCFRG research codes. The OLTARIS website is the successor to the SIREST website from the early 2000's. Modifications have been made to the code to enable easy maintenance, additions, and configuration management along with a more modern web interface. Overall, the code has been verified, tested, and modified to enable faster and more accurate assessments.

15. SUBJECT TERMS
Space radiation; Design tool; OLTARIS; Radiation effects

16. SECURITY CLASSIFICATION OF:			17. LIMITATION OF ABSTRACT	18. NUMBER OF PAGES	19a. NAME OF RESPONSIBLE PERSON
a. REPORT	b. ABSTRACT	c. THIS PAGE			STI Help Desk (email: help@sti.nasa.gov)
					19b. TELEPHONE NUMBER *(Include area code)*
U	U	U	UU	39	(443) 757-5802